SEMARAK ILMU PUBLISHING

CFD Letters

Journal homepage:
https://semarakilmu.com.my/journals/index.php/CFD_Letters/index
ISSN: 2180-1363

Structural Analysis of a First, Second and Third Generation Horizontal Axis Hydrokinetic Turbine

Cristian Cardona-Mancilla[1], Jorge Sierra-Del Rio[2,*], Alejandro Ruiz Sánchez[3], Edwin Correa Quintana[3], Carlos Arrieta González[4], Mario Luna-Del Risco[4]

[1] Department of Mechatronics Engineering, University ECCI, Medellín. Antioquia, Colombia
[2] Department of Mechanical Engineering, GIIAM, Pascual Bravo University Institution, Medellín. Antioquia, Colombia
[3] Department of Mechatronics Engineering, MATyER, Technological Metropolitan Institute, Medellín. Antioquia, Colombia
[4] Department of Engineering -GRINEN research group, Universidad de Medellin. Medellín, Colombia

ARTICLE INFO

Article history:
Received 25 May 2023
Received in revised form 21 June 2023
Accepted 18 July 2023
Available online 5 December 2023

Keywords:
CFD; Augmented; Diffuser; FEA; FSI; Renewable energy; River

ABSTRACT

The objective of this work is to evaluate through computational simulation the structural integrity of a horizontal axis hydrokinetic turbine (HAHKT) when using various geometric configurations of diffusers. This study was carried out by fluid - structure interaction (FSI) sing Ansys Workbench V18.2, coupling CFX and mechanical structural, in which a structural analysis was carried out based on the results obtained at the hydrodynamic level of a HAHKT composed of three blades with profile NREL S822, which was also analysed under the implementation of two geometric diffuser configurations. The maximum stresses in the blades increase of 27 % using the third-generation diffuser.

1. Introduction

The speed in which a river transports its waters is a constant and clean source of energy. Under the premise of taking advantage of it, but without having to build a large civil infrastructure such as that needed in large hydroelectric power plants, various types of turbines submerged in streams called hydrokinetic turbines have been developed, whose main objective is to generate electricity to power isolated rural populations or eventually deliver the energy produced to the electrical interconnection system as mentioned in some studies [1, 2]. This technology has several advantages in the renewable energy market; for example, the versatility to be used in various settings, where other technologies are inadequate. It allows the exploitation of the rivers, seas, and even artificial channels energy. Furthermore, this technology does not require large infrastructure constructions such as dams or power houses; since it does not require a large amount of accumulated water, the environmental impact is minimal as suggested by some references [3, 4]. However, because hydrokinetic turbines are still in development stage and due to the low energy density, that they allow to take advantage of, their economic feasibility must be carefully studied as shown in several

* *Corresponding author.*
E-mail address: jsierrad@pascualbravo.edu.co (Jorge Andrés Sierra Del Rio)

https://doi.org/10.37934/cfdl.16.1.7994

research projects [2, 5, 22]. Much of the literature related to the study of hydrokinetic turbines is based on computational techniques, among which the finite element method (FEM) stands out as a fast, economical, and reliable design tool compared to an experimental methodology [6, 7]

Different studies have been carried out with the aim of improving the efficiency of hydrokinetic turbines, varying both geometric and operational parameters. Among the geometric modifications are the effect of the number of [8] blades, the variation of their attack angle [9, 10] and the hydrodynamic profiles used for their constitution [11-13] . Another improvement that has been gaining weight is the implementation of increased diffusers in HAHKTs [14], reaching hydraulic efficiencies close to 90% with respect to the maximum extractable power of a fluid, established by the Betz limit [14, 15]. The increase generated by these devices is due to the radial opening that originates between the diffuser that surrounds the turbine and the diffuser attached to the rear of the turbine, adding energy to the fluid downstream of the turbine for moment conservation inside the volume study control, by allowing the entrance of the flow from the outside to the inside of the device, producing a drag force that helps to evacuate the fluid that passes through the turbine, reducing recirculation currents that are associated with energy losses in the fluid.

Although the implementation of increased diffusers allows to increase the efficiency of hydrokinetic turbines, the effect of the fluid on the blades generates an increase in the stress state that could cause a failure in the material. To avoid this, the effect of the flow on the structure must be determined, which can be done by implementing coupled simulations between the fluid and the structure (FSI), allowing to obtain the blade real stress state of the turbine.

Different studies related to the effect of the fluid on the blades of hydrokinetic turbines are reported in the literature, mainly determining the critical points of the turbine in terms of stress, in order to offer designers a valid criterion to reinforce these areas of the blades especially, which are obtained as a result of the previous studies [11, 16]. In addition to this, and understanding the advantages of the implementation of diffusers in hydrokinetic turbines, both numerical and experimental studies that validate the effect of the implementation of diffusers in hydrokinetic turbines on the structural integrity of the blades are presented, highlighting the results presented in Ref. [17, 21]. As a general result, a significant increase in the maximum stress in the blades, specifically near the blade attachment zone with the rotating shaft, is found in first- and second-generation turbines.

Recognizing the importance of determining the stress state to which the blades of a hydrokinetic turbine that implements a diffuser as a device to increase the capacity of electric power generation are subjected, in particular with the new geometry diffuser for the third generation turbine, this document presents as study objective: to determine the effect of implementing second and third generation diffusers on the stress state in the HAHKT blades, by computational simulation. In this work, the mechanical behaviour of a HAHKT is determined through simulation, with and without a diffuser, from the stresses and deformations presented to hydraulic loads of the fluid-structure interaction. The configuration of the structural analysis of the blades is presented as the main component of the hydrokinetic turbine, its main loading conditions are described, and the stresses and deformations presented by them are calculated, to verify their structural integrity when subjected to the operation conditions established in the hydrodynamic analysis.

2. Methodology

To carry out stress modelling in HAHKT, a fluid-structure interaction analysis (FSI) is used, in which the pressure fields exerted by the fluid on the structure are considered by a computational fluid analysis (CFD), allowing to estimate the stress and deformation state of the material through a

structural analysis. This FSI can be done in two ways, using one-way and two-ways coupling. For the first one, a CFD analysis of the fluid flow must be carried out initially, subsequently exporting the load obtained to a finite element analysis program to be applied, in this case, on the solid 3D model of the rotor. For bidirectional coupling, the procedure described above is performed in the first instance, with the difference that the results obtained in the FEM analysis are used as feedback from the CFD analysis, generating a closed loop that can be repeated as many times as necessary, until the desired convergence is reached. However, this last methodology requires a greater computational resource [18].

This study conducts an FSI analysis with unidirectional coupling of a HAHKT with and without diffuser, for which the turbine and diffusers were computably modelled, as well as the surrounding fluid in which they were submerged. To perform the FSI the ANSYS ® V18.2 program was used, and the methodology implemented is specified in the flowchart in Figure 1.

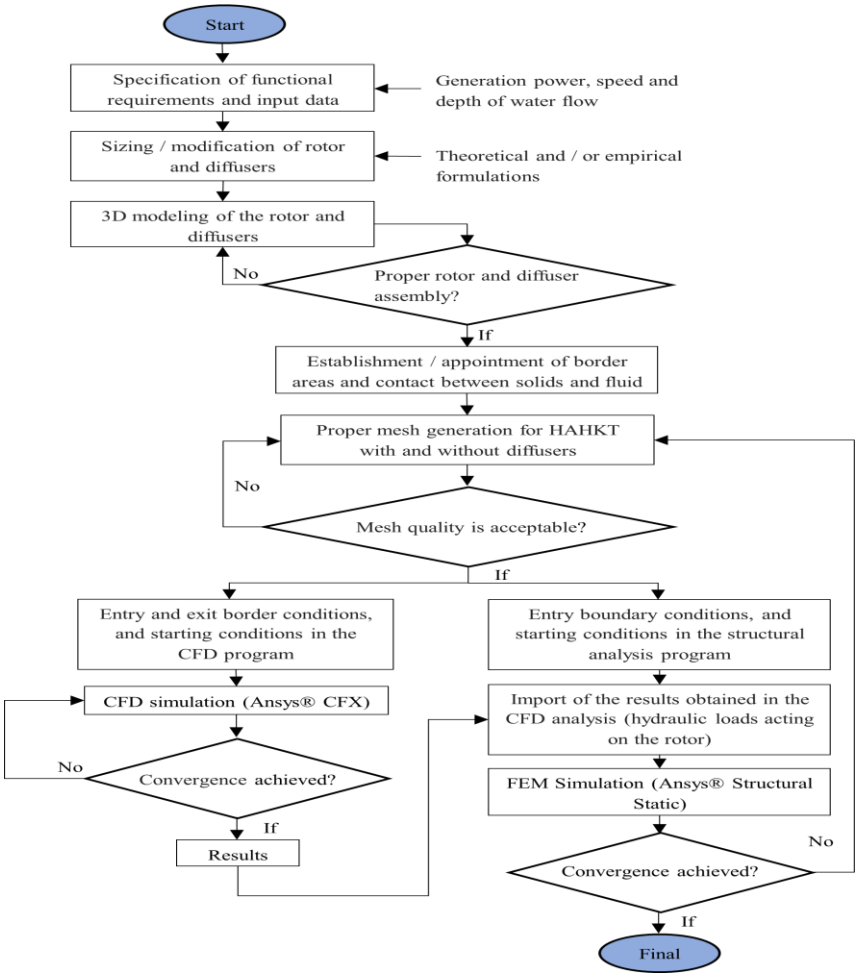

Fig. 1. Flowchart of the methodology used for the analysis of fluid-structural interaction implemented on the three-dimensional model of the HAHKT

2.1 CFD Modeling

To obtain the hydraulic load exerted on the rotor and the speeds distribution throughout the fluid domain, the CFD modeling methodology for the surrounding HAHKT fluid is used, as shown in Figure 1, and a brief detail of this modelling is presented in the following subsections.

2.1.1 Geometry model

This work was carried out considering the hydrodynamic models and results obtained in the article: "Computational Fluids Dynamics Analysis at First, Second and Third Hydrokinetics Turbine Generation" [19]. In which a 1 HP horizontal axis hydrokinetic turbine was designed for average speeds of Colombian rivers of 1.5 m/s. Which was constituted by a cube and three blades (Figure 2.a), the latter being made using the hydrodynamic profile NREL S822, also using two (2) diffuser configurations, which were implemented to improve the behaviour of the water fluid down the turbine.

For the design of the first diffuser (Figure 2.b), a profiled casing was implemented using the hydrodynamic profile NREL S822 previously used in the design of the blades of the hydrokinetic turbine, applying a scale of 3:1, guaranteeing that the turbine stayed inside the diffuser, along it. For the second geometric configuration of the diffuser, geometry similar to the third-generation hydrokinetic turbine (Figure 2.c) presented in the study carried out by Els and Junior [20] was used, which served as a form reference to develop a diffuser with said Constitution.

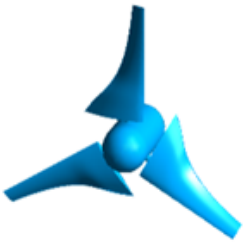

(a) Without diffuser (1st generation)

(b) With diffuser 1 (2nd generation)

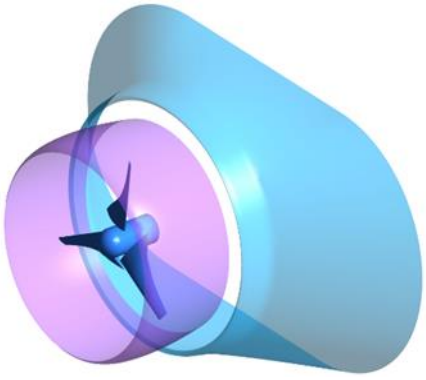

(c) With diffuser 2 (3rd generation)

Fig. 2. Detail design of HAHKT

2.1.2 Mesh generation

The meshing of the three three-dimensional models of the turbine with and without diffuser was performed using the Meshing® module of the ANSYS® V18.2 program, using unstructured meshes formed mainly by tetrahedral elements, using a proximity algorithm for the turbine without diffuser and curvature, and for the other models, a curvature algorithm. For all cases, a mesh relevance of +100 and a mesh dimensioning (Sizing) were applied on the trailing edge of the hydrodynamic profile of the turbine blade specifying a maximum size of 1 mm, in addition to using for the turbine without diffuser and with diffusers 1 and 2, respectively, a dimensional restructuring controlled by the parameters of minimum size (Min Size) of 5, 35 and 40 mm, maximum face (Max Phase Size) of 10, 45 and 50 mm, and maximum tetrahedron (Max Tet Size) of 20, 55 and 60 mm. These values were established considering the respective independence study of the mesh of the results, presenting percentages of change less than 4% of the torque generated by the turbine. The mesh metrics obtained in this process are found in Table 1.

Table 1
Mesh metrics of the CFD analysis performed on the turbine with and without diffuser

Models	Skewness, [Max.]	Orthogonal quality, [Max.]	Aspect radio, [Max.]	Number of nodes [10^6]
HKT without diffuser	0.8487	0.9979	12.521	3.67
HKT with diffuser 1	0.8678	0.9972	11.517	1.76
HKT with diffuser 2	0.8499	0.9987	17.105	3.62

2.1.3 Turbulence modelling

The meshed models are imported into the ANSYS® CFX module, in which the hydrodynamic analysis is performed under the operating conditions of the turbine, opting for the implementation of the k-ε turbulence model, due to its wide use in the literature by the good results presented when solving problems in which a fluid must pass through complex geometries. Being used for the analysis of the HAHKTs the continuity and Reynolds-averaged Navier-stokes equations, presented in Eq. (1) and Eq. (2), respectively [16]

$$\frac{\partial u_i}{\partial x_i} = 0 \tag{1}$$

$$\frac{\partial u_i}{\partial t} + u_j + \frac{\partial u_i}{\partial x_j} + \frac{1}{\rho}\frac{\partial \rho}{\partial x_i} - \frac{\partial}{\partial x_i}\left(v\left(\frac{\partial u_i}{\partial x_j} + \frac{\partial u_j}{\partial x_i}\right) - \tau_{ij}\right) = 0 \tag{2}$$

Where: u is the velocity, p is the pressure, ρ is the density, v is the kinematic viscosity and τ_{ij} is the Reynolds stress tensor.

2.1.4 Boundary conditions and CFD setup

Figure 3 shows the configuration of the boundary conditions of one of the analysed models, which, like the others, consists of a stationary volume, which corresponds to the volume of fluid external to the turbine and the diffuser, representing the river or water channel in which the device is submerged; and a rotating domain made up of the volume of fluid between the turbine and the diffuser. For all the modelled scenarios, a water flow inlet velocity of 1.5 m / s and a gauge pressure at the outlet of 0 Pa were used as initial parameters. Non-slip walls were established as limits of the

stationary domain, as well as the faces of the turbine and diffusers. An angular speed variation from 0 to 300 rpm, with increments of 10 rpm, was performed for all models.

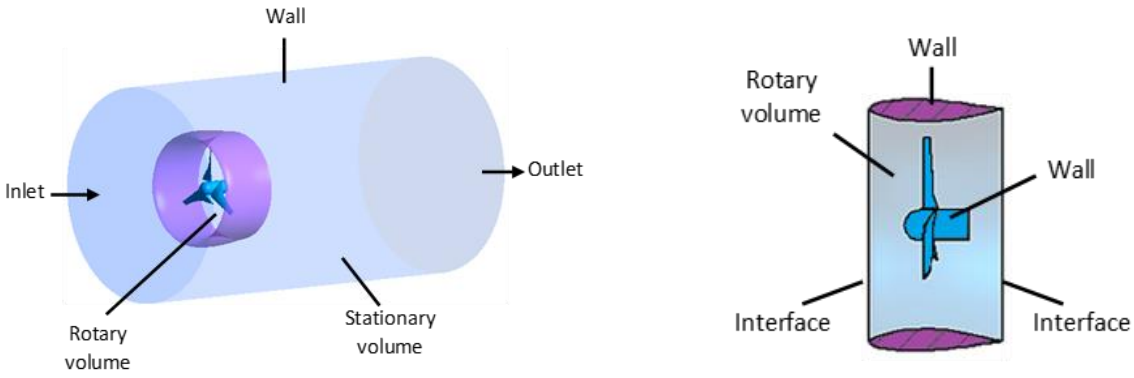

(a) Full volume (b) Rotating volume

Fig. 3. Definition of model boundaries

The CFD analysis of the models was carried out using the CFX module of the ANSYS® V18.2 program, which were configured in a transitional regime characterized by a total time of 4 s for the turbine without diffuser and 6 s for the turbine with diffuser. A passage time of 1.0E-02 s was used for all cases, guaranteeing maximum RMS values of 1.0E-04 as conservation criteria in conservation of mass and amount of movement. Water at 25 ° C was used as the working fluid and a k-ε turbulence model, which was selected according to the studies carried out by Chica *et al*., [6]. The interface between the walls of the stationary and the rotary volume was configured as "Frozen rotor" based on the study carried out by Kim *et al.,* [23] and the programming of a double precision study to reduce numerical errors.

The ANSYS® CFX post processor was used to calculate the field variables corresponding to the set of computational nodes of the analysed models, from which different types of graphs and contours could be obtained, acquiring greater relevance for the case studies, the velocity and pressure distribution within the fluid domain. Pressure data that was later used to power the structural static module. More details about the design, the measurements of each model, the mesh parameters, the simulation, and the results of the CFD analysis are specified in Ref. [19].

2.2 FEM Modelling

To verify the structural integrity of the hydrokinetic turbine, a rotor stress analysis is performed under the load conditions obtained in the CFD simulation, as shown in Figure 1. The structural analysis of the turbine with and without diffuser was performed in the Static-Structural module of the ANSYS® V18.2 program and a brief detail of the FEM modelling is presented in the following subsections.

2.2.1 3D geometry of solid model

The geometric treatment of the solid 3D models of the HAHKT with and without a diffuser, shown in previous sections (Figure 2), was carried out using the ANSYS® V18.2 geometry module, in which the bodies corresponding to the fluids, as well as the diffuser housings were suppressed, leaving only the solid bodies that will be subjected to structural analysis, being in this case the hydrokinetic turbine made up of the blades and the hub (Figure 4), since they are the most critical components.

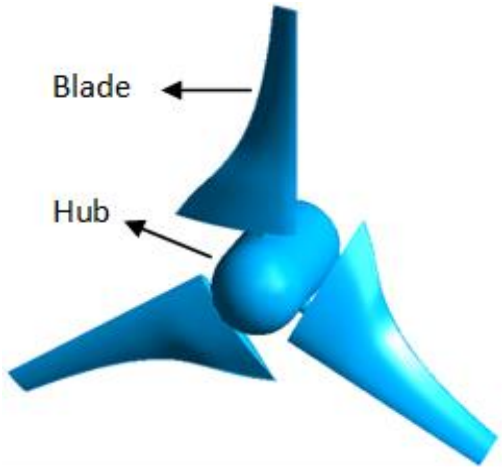

Fig. 4. Solid bodies of the model that will be subjected to structural analysis

2.2.2 Mesh generation

The process of discretizing the HAHKT control volumes was carried out in the Meshing® module of the ANSYS® V18.2 program. For the three models, an unstructured mechanical type tetrahedral mesh was established, with a function of proximity size and parameters of minimum size (Min Size) of 30 mm, maximum of face (Max Face Size) of 40 mm and maximum of the tetrahedron (Max Tet Size) of 50 mm, in addition to a face dimensioning (Face Sizing) on the blade surfaces of 2 mm and an edge dimensioning (Edge Sizing) on the trailing edge of the blade profile of 1 mm. To establish these dimensions, a mesh independence study was carried out, using the parameters described above, allowing various mesh refinements to be made using the effort generated on the turbine blades as a response variable, guaranteeing variations less than 4% compared to increases in the number of nodes, thus providing greater reliability of the results obtained (Figure 5). The mesh metrics obtained in this process are found in Table 2.

Table 2
Mesh metrics of the CFD analysis performed on the turbine with and without diffuser

Models	Number of mesh elements [10^6]	Number of nodes [10^6]
HKT without diffuser	2.26	3.33
HKT with diffuser 1	7.32	10.8
HKT with diffuser 2	5.36	7.93

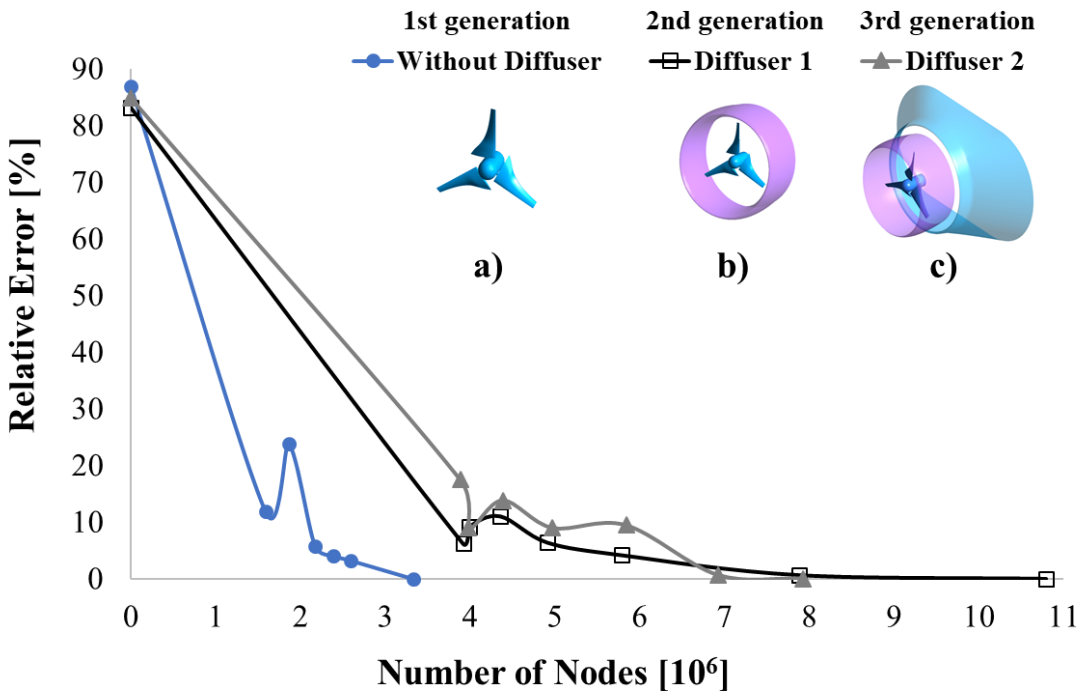

Fig. 5. Mesh independence study carried out for the structural analysis of HAHKT: a) without diffuser, b) with diffuser 1, and c) with diffuser 2

2.2.3 Loading and boundary conditions

Under normal operating conditions, HAHKTs are subject to loads produced by the pressure of the fluid flowing through the rotor, which, due to the relationship between the coefficient of lift and drag generated on the hydrodynamic profiles used in this type of turbines, allows the rotation of these. For this reason, the hydraulic load that is used on the solid domain implemented in the FEM simulation is obtained from the results obtained in the CFD analysis on the surrounding fluid, being imported in this case from the ANSYS® CFX module. To carry out the structural analysis of the three models, the boundary condition of the turbine is considered as follows: the axis of the turbine is established as a fixed support (Figure 6.a) and the hydraulic load obtained in the CFD analysis on the blades is applied (Figure 6.b). Finally proceeding to calculate the maximum von Mises effort.

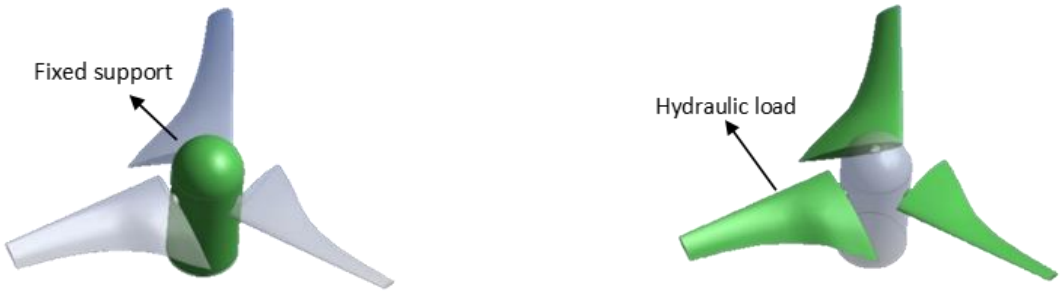

(a) Fixed support on the turbine shaft (b) Load distribution on the blades

Fig. 6. Boundary conditions established for the structural analysis of the HAHKT

2.2.4 Material

Given the high bending moments generated by the hydrodynamic forces on the turbine blades, it is necessary to establish for these, materials that have good mechanical properties (stiffness modulus, elastic modulus, high yield stress, among others). It should also be considered that the material has a high resistance to erosion and corrosion, due to the wear that water currents can cause on the blades when exposed for long periods of time in this type of environment [24] and more considering that HAHKTs can have a life cycle of more than 20 years [25]

Under these considerations and due to its good mechanical and chemical performance, this study was carried out using a CA-6NM martensitic stainless steel, composed of 13% Cr and 4% Ni, as it is widely used for the manufacture of hydraulic turbines due to its excellent mechanical properties, such as its good resistance to corrosion and erosion by cavitation [26]. Some of the mechanical properties of this material are presented in Table 3 according to commercial steel specifications [27], which are used in the process of configuring the setup of the FEM simulation.

Table 3
Mesh metrics of the CFD analysis performed on the turbine with and without diffuser

Material	Density (kg/m3)	Young's modulus (GPa)	Poisson coefficient	Ultimate stress (MPa)	Hardness (HB)	Resistance fatigue	Relative machinability (%)
Stainless steel CA-6NM	7700	206	0.288	560/950	220-320	Alta	90 [28]

3. Results

3.1 Comparison and Validation of Results

Despite the growing interest in the implementation of augmented diffusers in HAHKTs, there are no studies in the literature that apply an FSI analysis to these. Due to this and to compare and validate the results obtained here, a qualitative comparison is made between different studies with the objective to determine numerically the maximum stress and its location in HAHKTs. For this, the works carried out by Muñoz, Chiang, and De la Jara [29]; and Li, Hu, Chandrashekhara, Du, and Mishra [30], were considered, in which they analysed by CFD analysis a HAHKT on a small and medium scale, respectively.

Figure 7 presents some of the results obtained in the two studies that were taken as a reference base for the comparative analysis and validation of the results obtained in this work, where the critical position of the concentration of the supported stresses by the turbine blades is shown. Finding that, both for the two reference cases and for the three models analysed (Figure 8), the greatest stress achieved is given at the root of the blades, that is, in the area in which they join the cube. This is mainly since, in this area, a pivot point is generated that must withstand the bending moments caused by the stresses generated along the length of the blade, additionally torsional stresses occur due to the difference in pressure on the blade face with respect to the pivot axis, as shown in Figure 7. On the other hand, the reduction of area that occurs in this sector may also influence, which can be more easily evidenced in the models used in this study and the second case of comparison (Figure 11.b), due to the so-called phenomenon of stresses. These similarities at the structural level between the analysed models and the two cases taken as a reference base allow determining a coherent behaviour of the results obtained.

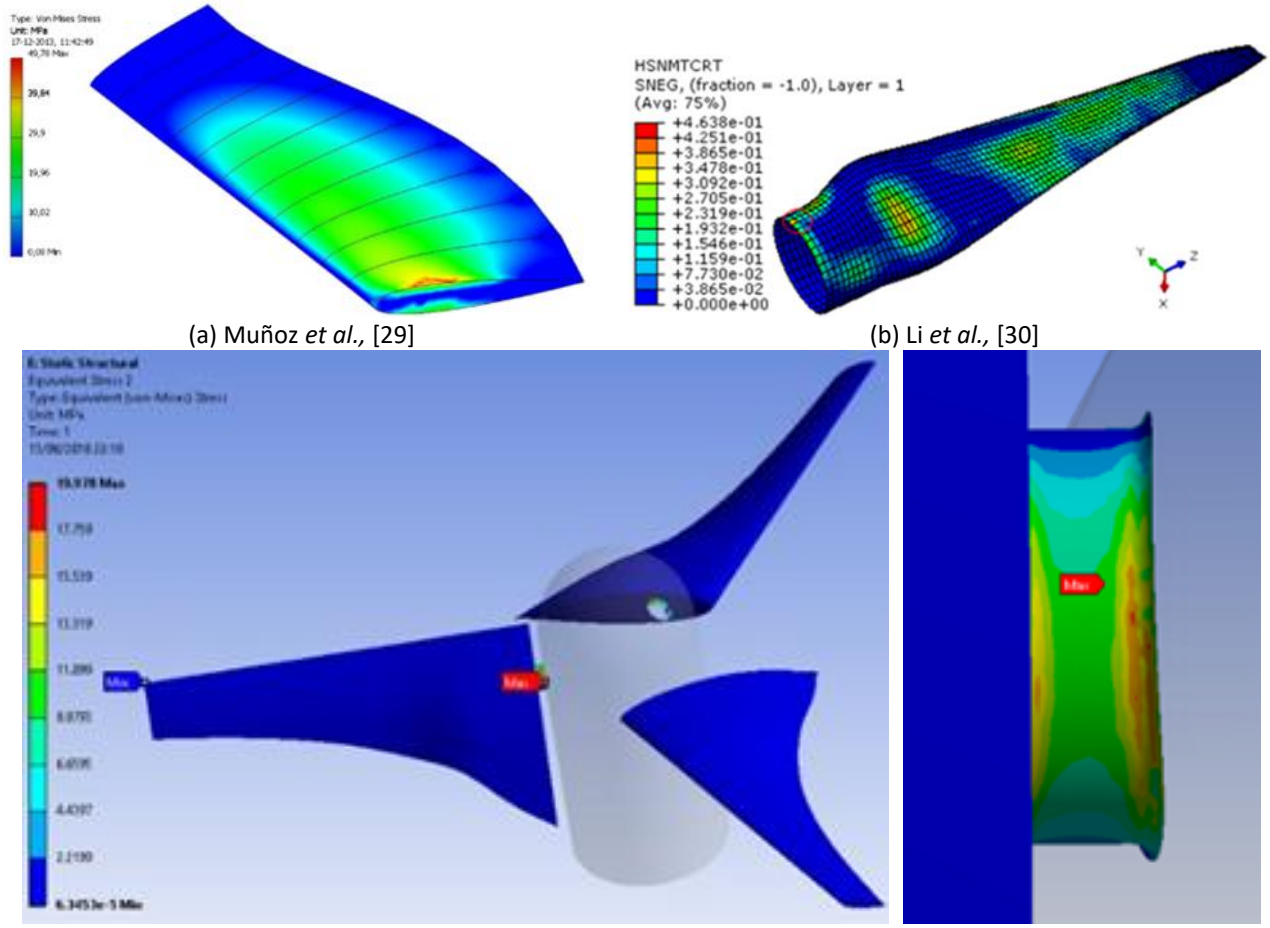

(a) Muñoz *et al.,* [29] (b) Li *et al.,* [30]

(c) Present study

Fig. 7. Critical position of the concentration of the stresses supported by the turbine blade in the studies

In the same way, comparing the numerical results of the similar first generation turbine (without diffuser) with the results reported by previous study [31], a difference of 0.57% is found for the Cp, max at TSR of 5.2, which allows validating the computational model for the first generation turbine. Once this case is validated, an acceptable degree of certainty is assumed for the Cp results for the second and third generation turbines.

Figure 8 shows the pressure distribution generated by hydrodynamic forces on the profile of the turbine blade without diffuser. The pressures include values between -3302 Pa and 1388 Pa. In the figure, the area of greatest pressure (1388 Pa) is on the upper area of the blade, near the leading edge of it, which is consistent because it is the region that comes into direct contact with the water at first, presenting a subsequent decrease in pressure as it moves away from this edge. On the other hand, the pressure difference presented on the upper face (upstream of the turbine) with respect to the pivot axis, causes the blade to rotate on its support, which must be absorbed by the blade clamping system. Additionally, there is a pressure difference between the upper and lower area of the blade with positive and negative values, respectively, reflecting a pressure drop downstream of the turbine that makes it possible to rotate. This behaviour is similar for all cases evaluated.

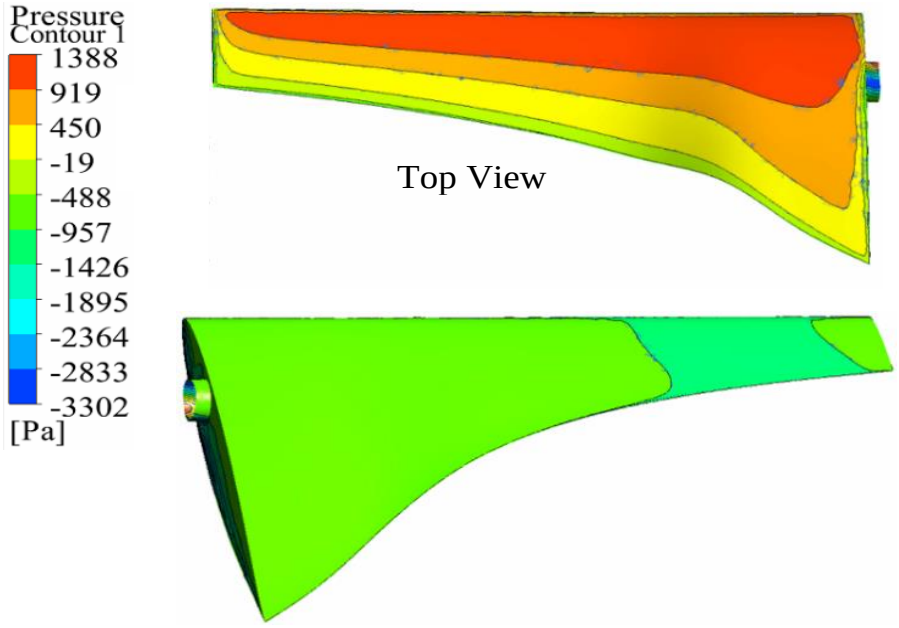

Fig. 8. Distribution of pressures generated by hydrodynamic forces on the profile of the hydrokinetic turbine blade without diffuser

Figure 9 shows a Von Mises equivalent stress contour to which the turbine blades are subjected with and without a diffuser. The maximum von Mises stress values were 15.73 MPa; 13.2 MPa and 19.98 MPa, for the turbine without diffuser and with diffusers 1 and 2, respectively. In all cases, the maximum stress supported by the blades is close to its root, specifically on the axis that connects them to the hub. In this figure, an approach (right side) of the area of interest is shown, which shows that, in all the cases analysed, the greatest stresses are found in this connection region. However, the safety factor for the blade of the third-generation diffuser (diffuser 2) implementation is 27, which guarantees the integrity of the blades before the effort exerted by the fluid.

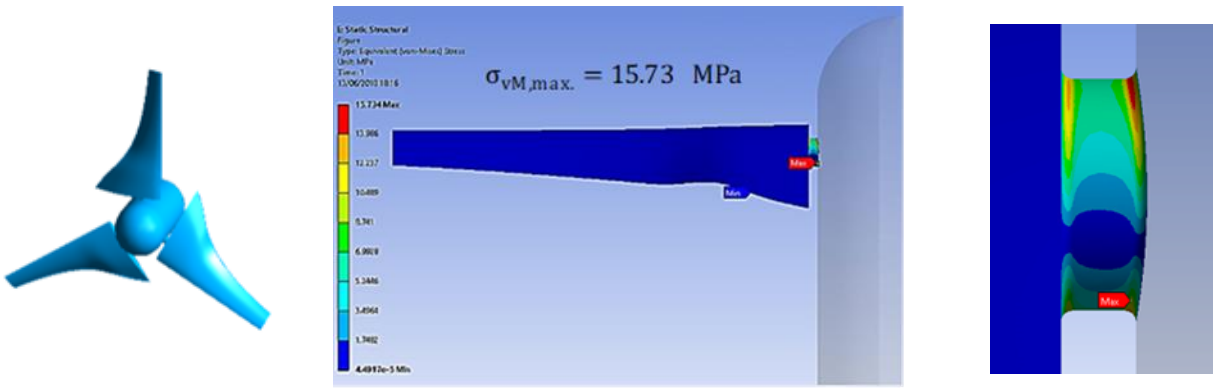

(a) Without diffuser (1st generation)

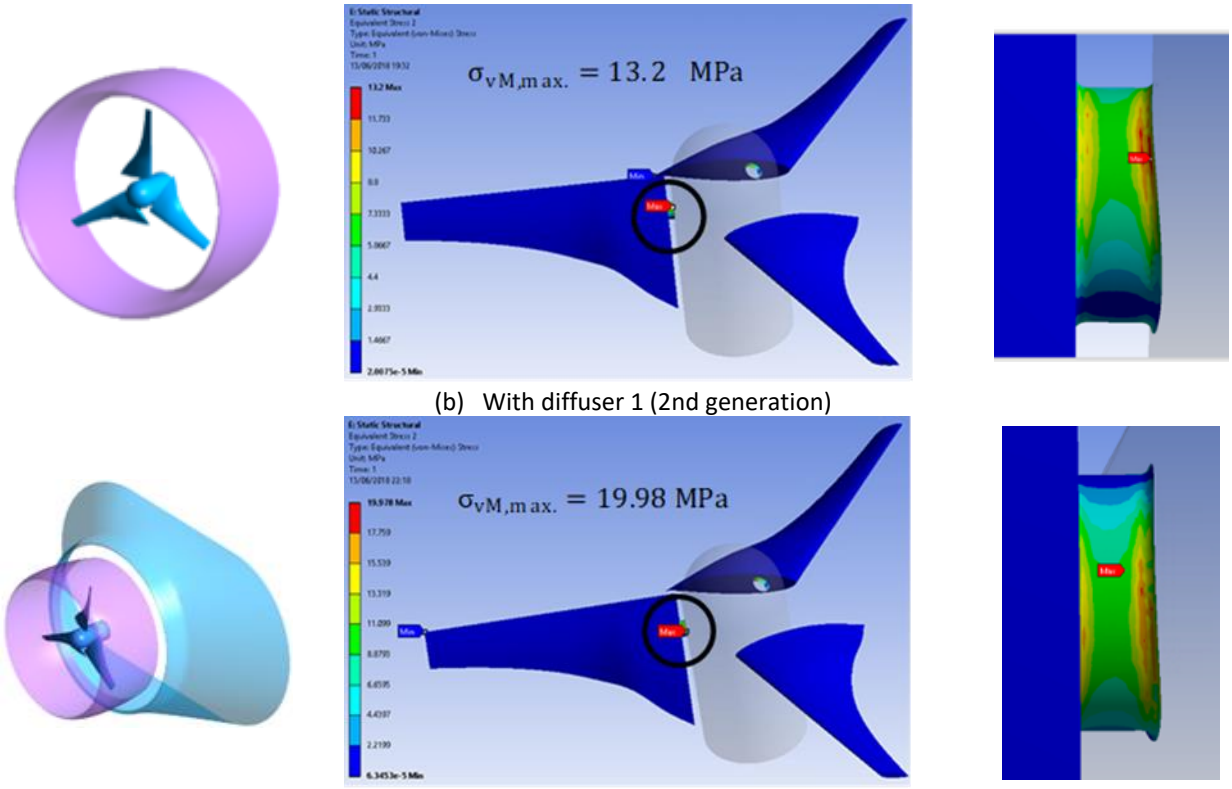

(b) With diffuser 1 (2nd generation)

(c) With diffuser 2 (3rd generation)

Fig. 9. von Mises stresses to which the turbine blades are subjected

Figure 10 shows the total deformation obtained in the structural analysis for the turbine with and without diffuser. The maximal deformations in the blades were values 0.067 mm; 0.069 mm 0.107 mm, for the turbine without diffuser and with diffuser 1 and 2, respectively. The turbine with the third-generation diffuser (diffuser 2) presents an increase of 59.7 and 55.1% of the total deformation of the blade with respect to the deformation presented by the turbine without diffuser and with the second-generation diffuser (diffuser 1), respectively. However, it is evident that the implementation of some types of diffusers, especially when they are made up of devices located downstream of the turbine, can increase the deformation of the blades, given that it is linked to the supported stresses, the which in turn are affected by the increased pressures that this type of mechanism can bring about at the hydrodynamic level. Even so, the maximum deformation presented by the material is relatively low and does not represent a great influence on the structural integrity of the blade. This oversizing is for the purpose of ensuring primarily design geometry. This result shows the feasibility of manufacturing hollow blades, which allow to reduce the weight of the turbine, the costs of materials and manufacturing processes, as well as the robustness of the different mechanical components such as shafts, bearings, bolts, among others, which would allow increasing the efficiency of the turbine by reducing the mechanical losses mainly associated with friction mechanisms between mechanical components.

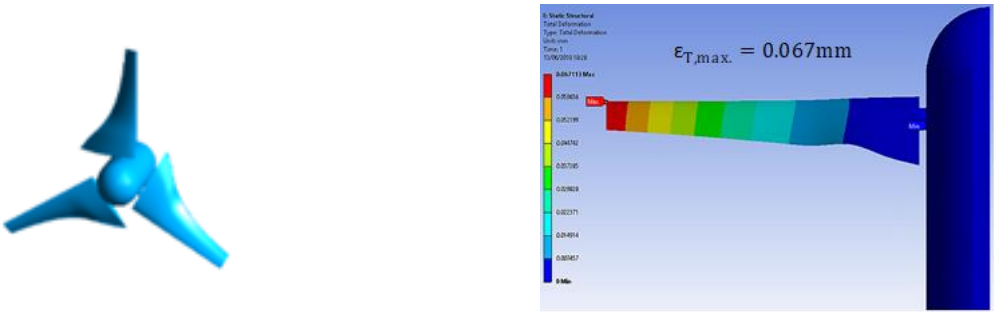

(a) Without diffuser (1st generation)

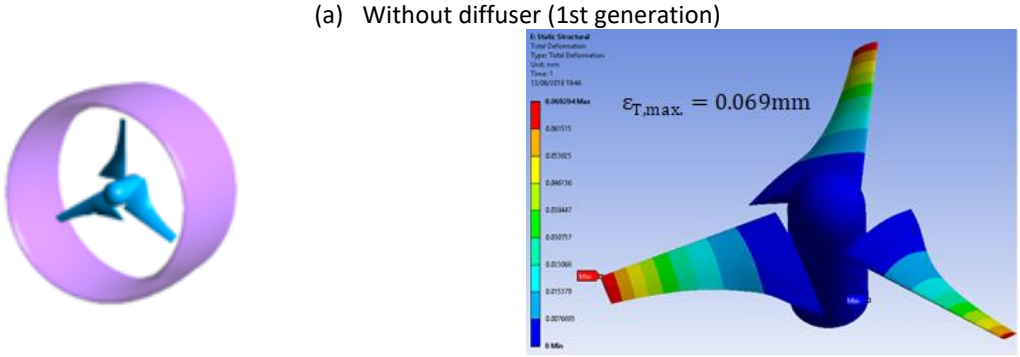

(b) With diffuser 1 (2nd generation)

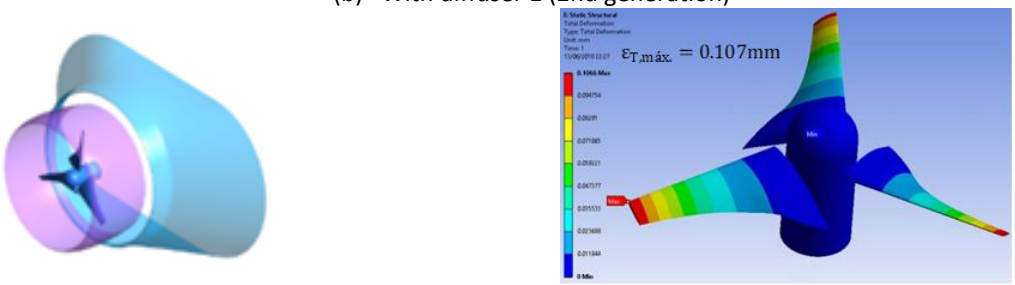

(c) With diffuser 2 (3rd generation)

Fig. 10. Total deformation presented by the turbine blades: (a) without diffuser, (b) with diffuser 1 and (c) with diff user 2

Figure 11 shows the variation of the power coefficient, Cp, and of the state of equivalent stresses by von Mises to which the blades of the three analysed models of the HAHKT are subjected. They comprise dimensionless values between 0.285 and 0.487, at TSR values 5.23 and 4.97, for the first and third generation turbine respectively, and the stresses between 13.2 and 19.98 MPa for the second and third generation models respectively. The results show a slight increase in the Cp for the second-generation turbine with respect to the turbine without diffuser, which is because generated by the mechanism downstream of the turbine by reducing recirculation and stagnation of water, accelerating the fluid to leave this critical area more quickly, thus reducing its attempt to prevent the rotor from turning correctly. In the same way, this second model also presents in relation to its predecessor a slight drop in the stresses generated on the turbine blades, given that the profiled diffuser channels the fluid upstream of the turbine, increasing the speed and decreasing, due to the Bernoulli principle, the pressure in this area, which is reflected in the reduction of the stresses supported by the blades. For its part, the third generation turbine shows an increase in Cp, which is firstly due to what was previously stated for the increase of this coefficient in the second generation turbine, given that this model is used as one of the two diffusers that make up this mechanism, and, secondly, the diffuser located downstream of the turbine that generates a new acceleration on the fluid that has passed through the turbine, allowing a better evacuation of the same, minimizing to a greater extent the interference that generates the recirculating water on the rotation of the rotor,

so the implementation of this device downstream of the turbine becomes the element that brings the greatest benefit in relation to the reduction of losses associated with the phenomenon of recirculation. Likewise, the suction generated by the second diffuser downstream of the turbine, causes the blades to be subjected to a greater stress. It is also evident that, when using the third-generation turbine, a similar trend of change can be found between the behaviour of the Cp curves and the stresses supported, allowing to establish a proportional growth relationship between them.

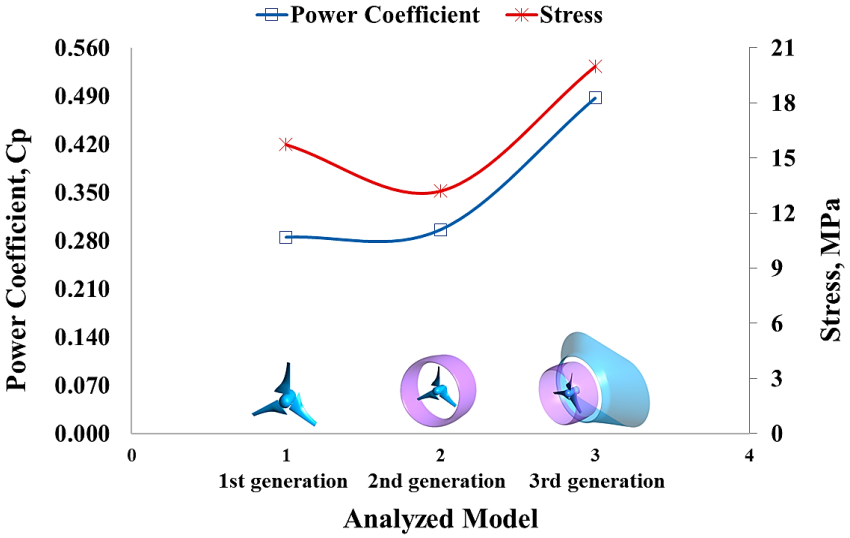

Fig. 11. Variation of the power coefficient (Cp) and of the equivalent stress by von Mises present in the first, second and third generation HAHKT

4. Conclusions

A structural analysis was used on the turbine, using the hydrodynamic loads obtained in the fluid-dynamic simulation for the models with and without a diffuser, which allowed determining that the maximum stresses supported by the blades did not exceed in any case the mechanical resistance of the selected material (CA-6NM stainless steel), presenting deformations less than 0.107 mm, which guarantees the structural integrity of the turbine when subjected to the operating conditions established in this work. These results show an oversizing in the material used for this type of mechanisms, for which the viability of manufacturing hollow blades is established, allowing to reduce both the weight of the turbine, as well as the cost of materials and manufacturing processes, which also leads to a decrease in friction between the mechanical components used in the transmission of movement, thus allowing increased efficiency of the turbine.

The results obtained in the structural simulation reflect similar behaviours to those presented by other authors [29-30], allowing greater reliability to the data found.

Acknowledgement

We would like to express our thanks to our colleagues from [Department of Mechatronics and Electromechanics/Metropolitan Technological Institute] who provided insight and expertise that greatly assisted the research.

References

[1] Aguilar, Jonathan, Ainhoa Rubio-Clemente, Laura Velasquez, and Edwin Chica. "Design and optimization of a multi-element hydrofoil for a horizontal-axis hydrokinetic turbine." *Energies* 12, no. 24 (2019): 4679. https://doi.org/10.3390/en12244679

[2] Tigabu, Muluken Temesgen, Dawit Diriba Guta, and Bimrew Tamrat Admasu. "Economics of hydro-kinetic turbine for off-grid application: A case study of Gumara River, Upper Blue Nile, Amhara, Ethiopia." *International Journal of Renewable Energy Research (IJRER)* 9, no. 3 (2019): 1368-1375.

[3] Al-Dabbagh, Mohammad A., and Mehmet Ishak Yuce. "Simulation and comparison of helical and straight-bladed hydrokinetic turbines." *International Journal of Renewable Energy Research* 8, no. 1 (2018): 504-513.doi: https://doi.org/10.20508/ijrer.v8i1.6697.g7345.

[4] Yuce, M. Ishak, and Abdullah Muratoglu. "Hydrokinetic energy conversion systems: A technology status review." *Renewable and Sustainable Energy Reviews* 43 (2015): 72-82.doi: 10.1016/j.rser.2014.10.037.

[5] Chica, E., F. Perez, A. Rubio-Clemente, and S. Agudelo. "Design of a hydrokinetic turbine." *WIT Transactions on Ecology and the Environment* 195 (2015): 137-148.doi: 10.2495/ESUS150121.

[6] O'Brien, J. M., T. M. Young, D. C. O'Mahoney, and P. C. Griffin. "Horizontal axis wind turbine research: A review of commercial CFD, FE codes and experimental practices." *Progress in Aerospace Sciences* 92 (2017): 1-24. doi: 10.1016/j.paerosci.2017.05.001.

[7] Liu, Xin, Yongyao Luo, Bryan W. Karney, and Weizheng Wang. "A selected literature review of efficiency improvements in hydraulic turbines." *Renewable and Sustainable Energy Reviews* 51 (2015): 18-28.doi: 10.1016/j.rser.2015.06.023.

[8] Alipour, Ramin, Roozbeh Alipour, Farhad Fardian, Seyed Saeid Rahimian Koloor, and Michal Petrů. "Performance improvement of a new proposed Savonius hydrokinetic turbine: a numerical investigation." *Energy Reports* 6 (2020): 3051-3066.doi: 10.1016/j.egyr.2020.10.072.

[9] Pourmahdavi, Maryam, and Shahram Derakhshan. "Numerical study into the effect of working environment on energy extraction performance of tandem arranged flapping foils." *International Journal of Renewable Energy Research (IJRER)* 8, no. 3 (2018): 1604-1611., doi: https://doi.org/10.20508/ijrer.v8i3.7844.g7459.

[10] Alipour, Ramin, Roozbeh Alipour, Farhad Fardian, and Mohammad Hossein Tahan. "Optimum performance of a horizontal axis tidal current turbine: A numerical parametric study and experimental validation." *Energy Conversion and Management* 258 (2022): 115533. doi: 10.1016/j.enconman.2022.115533.

[11] Chica, Edwin, and Ainhoa Rubio-Clemente. *Design of zero head turbines for power generation*. London, UK: IntechOpen, 2017. doi: 10.5772/66907.

[12] Abdolahifar, Abolfazl, Mahdi Azizi, and Amir Zanj. "Flow structure and performance analysis of Darrieus vertical axis turbines with swept blades: A critical case study on V-shaped blades." *Ocean Engineering* 280 (2023): 114857, doi: 10.1016/j.oceaneng.2023.114857.

[13] Chaudhari, Vimal N., and Samip P. Shah. "Numerical investigation on the performance of an innovative Airfoil-Bladed Savonius Hydrokinetic Turbine (ABSHKT) with deflector." *International Journal of Thermofluids* 17 (2023): 100279. doi: 10.1016/j.ijft.2023.100279.

[14] Nunes, Matheus M., Antonio CP Brasil Junior, and Taygoara F. Oliveira. "Systematic review of diffuser-augmented horizontal-axis turbines." *Renewable and Sustainable Energy Reviews* 133 (2020): 110075. doi: 10.1016/j.rser.2020.110075.

[15] van Els, Rudi Henri, and Antonio Cesar Pinho Brasil Junior. "The Brazilian experience with hydrokinetic turbines." *Energy Procedia* 75 (2015): 259-264., doi: 10.1016/j.egypro.2015.07.328.

[16] Kolekar, Nitin, and Arindam Banerjee. "A coupled hydro-structural design optimization for hydrokinetic turbines." *Journal of renewable and sustainable energy* 5, no. 5 (2013), doi: 10.1063/1.4826882.

[17] Kumar, Dinesh, and Shibayan Sarkar. "Modeling of flow-induced stress on helical Savonius hydrokinetic turbine with the effect of augmentation technique at different operating conditions." *Renewable Energy* 111 (2017): 740-748, doi: 10.1016/j.renene.2017.05.006.

[18] ESSS, "Interacción Fluido-Estructura". (2016). https://www.esss.co/es/blog/interaccion-fluido-estructura/ (accessed Feb. 09, 2020).

[19] C.-M. Cristian, S.-D. R. Jorge, and H.-Z. Diego. (2018). "Computational Fluids Dynamics Analysis at First, Second and Third Hydrokinetics Turbine Generation," *Indian J Sci Technol*, vol. 11, no. 36, pp. 1–8, doi: 10.17485/ijst/2018/v11i36/129278.

[20] L. Piancastelli, R. V Clarke, and S. Cassani. (2017). "DIFFUSER AUGMENTEDRUN THE RIVER AND TIDAL PICO-HYDROPOWER GENERATION SYSTEM," vol. 12, no. 8. Available: http://www.arpnjournals.org/jeas/research_papers/rp_2017/jeas_0417_5957.pdf

[21] Kumar, Dinesh, and Shibayan Sarkar. "Modeling of flow-induced stress on helical Savonius hydrokinetic turbine with the effect of augmentation technique at different operating conditions." *Renewable Energy* 111 (2017): 740-748, doi: 10.1016/j.renene.2017.05.006.

[22] Chica, E., F. Perez, A. Rubio-Clemente, and S. Agudelo. "Design of a hydrokinetic turbine." *WIT Transactions on Ecology and the Environment* 195 (2015): 137-148. Doi: 10.2495/ESUS150121

[23] Kim, Seung-Jun, Patrick Mark Singh, Beom-Soo Hyun, Young-Ho Lee, and Young-Do Choi. "A study on the floating bridge type horizontal axis tidal current turbine for energy independent islands in Korea." *Renewable Energy* 112 (2017): 35-43., doi: 10.1016/j.renene.2017.05.025.

[24] Khaled, Fatima, Sylvain Guillou, Yann Méar, and Ferhat Hadri. "Impact of the blockage ratio on the transport of sediment in the presence of a hydrokinetic turbine: Numerical modeling of the interaction sediment and turbine." *International Journal of Sediment Research* 36, no. 6 (2021): 696-710, doi: 10.1016/j.ijsrc.2021.02.003.

[25] Kusakana, K., and H. J. Vermaak. "Cost and performance evaluation of hydrokinetic-diesel hybrid systems." *Energy procedia* 61 (2014): 2439-2442, doi: 10.1016/j.egypro.2014.12.019.

[26] F. Foroozmehr, "Ductile Fracture of 13% Cr-4% Ni Martensitic Stainless Steels Used in Hydraulic Turbine Welded Runners," École Polytechnique de Montréal, 2017. [Online]. Available: https://publications.polymtl.ca/2770/

[27] "http://www.matweb.com/ ."

[28] "https://www.sandvik.coromant.com/es-es/knowledge/materials/workpiece_materials/iso_m_stainless_steel/pages/default.aspx."

[29] Muñoz, A. H., L. E. Chiang, and E. A. De la Jara. "A design tool and fabrication guidelines for small low cost horizontal axis hydrokinetic turbines." *Energy for Sustainable Development* 22 (2014): 21-33. doi: 10.1016/j.esd.2014.05.003.

[30] Li, H., Zhongxu Hu, K. Chandrashekhara, Xiaoping Du, and R. Mishra. "Reliability-based fatigue life investigation for a medium-scale composite hydrokinetic turbine blade." *Ocean Engineering* 89 (2014): 230-242.doi: 10.1016/j.oceaneng.2014.08.006.

[31] F. Jing, W. Ma, L. Zhang, S. Wang, and X. Wang. (2017). "Experimental study of hydrodynamic performance of full-scale horizontal axis tidal current turbine," *Journal of Hydrodynamics*, vol. 29, no. 1, pp. 109–117, doi: 10.1016/S1001-6058(16)60722-9.